Available online at www.sciencedirect.com

SciVerse ScienceDirect

Ceramics International 39 (2013) 7693–7701

CERAMICS INTERNATIONAL

www.elsevier.com/locate/ceramint

Ion induced modification of bandgap and CIE parameters in $Y_2O_3:Dy^{3+}$ phosphor

S. Som[a], S.K. Sharma[a,*], S.P. Lochab[b]

[a]Department of Applied Physics, Indian School of Mines, Dhanbad 826004, India
[b]Inter University Accelerator Centre, New Delhi 110067, India

Received 1 February 2013; received in revised form 4 February 2013; accepted 10 March 2013
Available online 19 March 2013

Abstract

This paper reports the comparative investigation on structural and optical modifications of $Y_2O_3:Dy^{3+}$ phosphor after 150 MeV Ni^{7+} and 120 MeV Ag^{9+} swift heavy ions irradiation in the fluence range 1×10^{11}–1×10^{13} ions/cm^2. XRD and TEM studies confirm the loss of crystallinity of ion irradiated phosphors. Diffuse reflectance spectrum shows a blue shift in the absorption band resulting in an increase in band gap after ion irradiation. An increase in the intensity of photoluminescence peaks without any shift in the peak positions was observed with ion fluence. The color coordinates of ion irradiated phosphors approach the white light region with the increase of ion fluence.

Keywords: Phosphor; Swift heavy ion; Bandgap; CIE parameter

1. Introduction

Swift heavy ion (SHI) irradiation is a unique post-synthesis treatment due to its ability to modify the material's properties [1]. When swift heavy ion passes through materials, it suffers a significant electronic energy loss and high energy deposition which results in the increase in pressure and temperature inside the target material. These non-equilibrium conditions further help the system in achieving unique properties [2]. In case of insulators/ phosphors, this energy deposition may lead to the production of new color centers, point defects and rearrangement of trapping/luminescent centers which may modify the morphological, optical and optoelectronic properties of materials [3]. Inorganic oxide materials have been found to be sensitive to the effects induced by electronic energy loss of swift heavy ions. In the past decades, extensive research works have been carried out on the structural, optical and electronic modification of inorganic oxide phosphors after swift heavy ion irradiation [4,5].

Dysprosium doped yttrium oxide plays an important role in modern display technology due to their high luminescence efficiency with good thermal and chemical stability [6]. The brightness, resolution of color emission and optical parameters of this phosphor are markedly influenced by the swift heavy ion irradiation [7]. The creation of defects and their curing depends on the ion beam parameters such as energy loss of ions in the material, ion fluence and ion species [8]. Since irradiation can cause the creation of defects as well as their reordering in the system, it is imperative to have a comprehensive study of the effects of irradiation with a variety of ions in different fluence and energy ranges. With this objective, the present work was carried out on optical modification of $Y_2O_3:Dy^{3+}$ phosphor after the irradiation by different species of ions like Ni and Ag for varying ion fluences. To the best of our knowledge, the effect of swift heavy ion on the optical properties of dysprosium doped yttrium oxide phosphor is reported first time.

In the present studies, 150 MeV Ni^{7+} and 120 MeV Ag^{9+} ions were used for the irradiation purpose in the fluence range 1×10^{11}–1×10^{13} ions/cm^2. The irradiated phosphors were characterized by X-Ray diffraction (XRD), transmission electron microscopy (TEM), diffuse reflectance (DR) and photoluminescence (PL) studies and different optical parameters

*Corresponding author. Tel.: +91 3262235412; fax: +91 3262296563.
E-mail addresses: sksharma.ism@gmail.com.
sksharma_ism@yahoo.co.in (S.K. Sharma).

0272-8842/$ - see front matter © 2013 Elsevier Ltd and Techna Group S.r.l. All rights reserved.
http://dx.doi.org/10.1016/j.ceramint.2013.03.022

were calculated for virgin and ion irradiated phosphors. An attempt was made to compare the results of optical and luminescence studies of Y_2O_3:Dy^{3+} after ion irradiation.

2. Experimental

Dy doped Y_2O_3 phosphor was prepared by the combustion synthesis method using dysprosium oxide (Dy_2O_3), yttrium oxide (Y_2O_3), nitric acid (HNO_3) and urea ($CO(NH_2)_2$) as starting raw materials. The stock solutions of $Y(NO_3)_3$ and Dy $(NO_3)_3$ were prepared by dissolving Y_2O_3 and Dy_2O_3 in nitric acid and diluting with deionized water. The Dy doped sample was prepared by mixing $Y(NO_3)_3$ and $Dy(NO_3)_3$ according to the formula $(Y_{1-x}Dy_x)_2O_3$ ($x=0.05$) in a beaker. A suitable amount of urea was added to the mixture of the nitrate solution keeping urea to metal nitrate molar ratio as 2.5 [9]. The mixture was then dissolved properly to achieve a uniform solution and dried by heating at 80 °C using magnetic stirrer. Finally, the solid residue was transferred to silica crucible and heated at 600 °C in a furnace for an hour. The synthesis reaction [9] was

$$(2-2x)Y(NO_3)_3+2xDy(NO_3)_3+5(NH_2)_2CO\rightarrow(Y_{1-x}Dy_x)_2O_3+5CO_2+8N_2+10H_2O$$

For swift heavy ion (SHI) irradiation, the 15UD pelletron of Inter University Accelerator Centre (IUAC), New Delhi was used. Details regarding the SHI irradiation are reported elsewhere [3]. As the range of 150 MeV Ni^{7+} and 120 MeV Ag^{9+} ions inside the powder phosphor calculated using SRIM (Stopping and Range of Ions in Matter) computer program [10] was in micrometer range and it was not possible to make a pellet less than this range, a special type of arrangement was used for irradiating the powder phosphors instead of pellets. A strip with five holes of diameter 1 cm and inner thickness 0.5 mm were used. One side of the strip was covered with the silver foil and a suitable quantity of powder depending on the projectile range was put into the holes on the other side of the strip and was gently pressed with a solid cylinder of same diameter, so that it does not fall out from the strip. The strip was then carefully mounted on the sample holder having four faces fitted on the rectangular ladder of a scattering chamber connected to a beam line.

The ladder can be moved up-down or rotated about the vertical axis in order to bring the samples into the path of ion beam for irradiation. A pressure of 10^{-6} Torr was maintained inside the chamber during ion irradiation. After irradiating a sample to the desired fluence, the beam was turned off and a new sample was brought into the position for irradiation.

The variation of electronic/nuclear energy loss with beam energy [10] as calculated from the SRIM program is shown in Fig. 1. It shows that electronic energy loss (S_e) in Y_2O_3:Dy phosphor is maximum at around 150 MeV energy of Ni^{7+} and around 120 MeV energy of Ag^{9+} and nuclear energy loss (S_n) is negligible. This large electronic energy loss is responsible for the creation of new color centers, point defects and rearrangement of trapping/luminescent centers [11] thus modifying the optical and luminescence properties to a large extent. The S_e was calculated to be 22.66 and 43.78 MeV mg/cm^2 for 150 MeV Ni^{7+} ions and 120 MeV Ag^{9+} ions respectively. The greater S_e value for Ag^{9+} ion suggests the creation of more number of new color centers and point defects.

X-Ray diffractogram of virgin and ion irradiated phosphors were recorded in a wide range of Bragg angle 2θ ($15^\circ\leq 2\theta\leq 85^\circ$) using Bruker D8 Focus with Cu target radiation ($\lambda=0.154056$ nm). The morphology and crystallite size of the phosphors were determined by JEOL make JEM-2100 transmission electron microscope (TEM). The diffuse reflectance (DR) spectra were recorded using Perkin-Elmer make Lambda 35, UV–vis Spectrophotometer fitted with integrating sphere assembly in the wavelength range 190–800 nm. The photoluminescence studies were carried out on Hitachi make fluorescence Spectrophotometer F-2500 in the range 220–650 nm. All these studies were carried out at room temperature.

3. Results and discussions

3.1. Phase identification and morphology

3.1.1. X-Ray diffraction

Fig. 2(a) shows the X-ray diffraction pattern of the virgin and ion irradiated Dy^{3+} doped Y_2O_3 phosphors. The XRD peaks of virgin phosphor were identified and indexed according to the JCPDS file No. 83-0927 of Y_2O_3 [12]. The sharp and single diffraction peaks of the XRD pattern confirm the formation of single phase compound. No peaks were observed due to Dy dopant indicating that the incorporation of Dy^{3+} into the Y_2O_3 lattice does not influence the crystal structure. The effect of 150 MeV Ni^{7+} and 120 MeV Ag^{9+} ion irradiations for different ion fluences 1×10^{11} ions/cm^2 and 1×10^{13} ions/cm^2 in the XRD pattern of Dy^{3+} doped Y_2O_3 phosphors are shown in this figure. The figure shows that after ion irradiation, the peaks shifted toward lower angle side. Moreover, the full width at half maxima (FWHM) increases and the intensity of the peak decreases with the increase in ion fluences. Both the facts indicate the loss of crystallinity of the phosphors after ion irradiation [13]. No new peak was observed after ion irradiation indicating no change in phase of the phosphor. The loss of crystallinity was observed to be more for Ag ion irradiated phosphor than Ni ion irradiated phosphor. This indicates that Ag ion is more effective than Ni ion for the decrystallization of the phosphor.

3.1.2. Rietveld refinement

A structural refinement by the Rietveld method [14] using Fullprof Program [15] was performed to analyze the structure and unit cell of the prepared virgin phosphor. Fig. 2(b) and Table 1 represent the structural refinement results for virgin Y_2O_3:Dy^{3+} phosphor. The results indicate good agreement between the observed and calculated XRD patterns (Fig. 2(b)). The quality of structural refinement data [12] was checked by measuring two parameters called Bragg's contribution (χ^2) and goodness of fit (GOF). For perfect refinement, the χ^2 must be

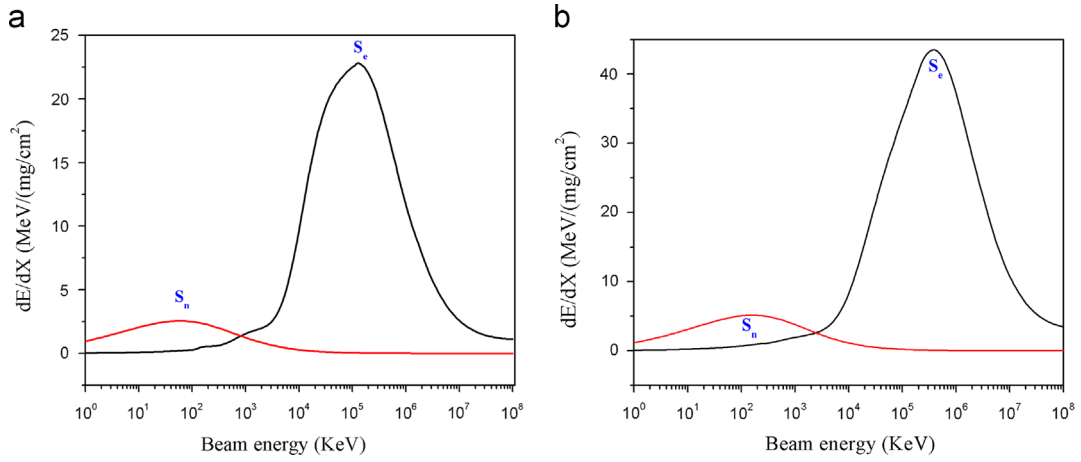

Fig. 1. Plot of energy loss of Ni^{7+} and Ag^{9+}-ions in Y_2O_3:Dy^{3+} phosphor.

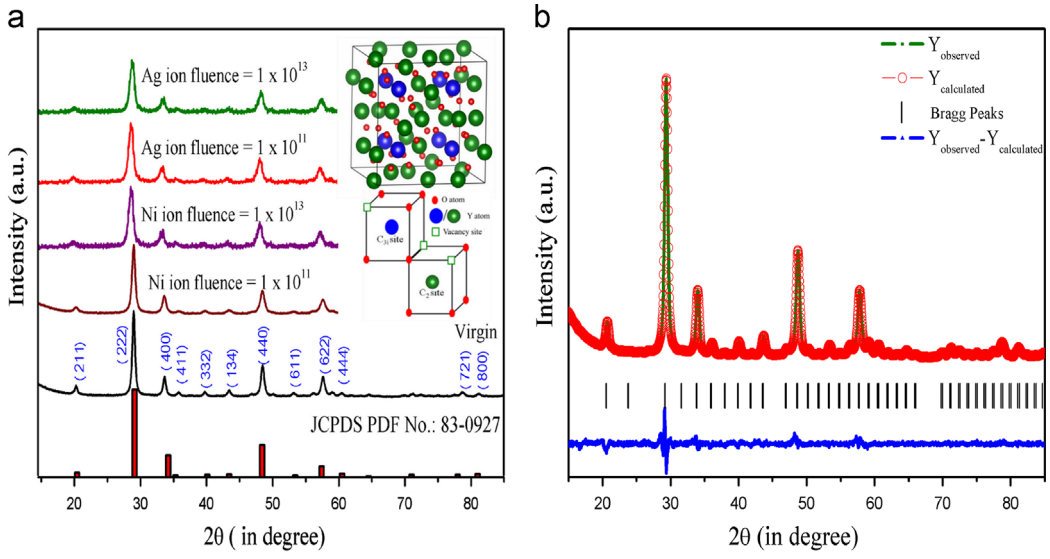

Fig. 2. (a) XRD Spectra of virgin and ion irradiated and (b) Rietveld refinement pattern of Y_2O_3:Dy^{3+} phosphors.

Table 1
Refinement parameters of virgin Y_2O_3:Dy^{3+} phosphors.

Phosphors	Atom	*x*	*y*	*z*	Lattice constants
Virgin Y_2O_3:Dy^{3+}	Y1	0.250	0.250	0.250	10.61 Å
	Y2	0.967	0.000	0.250	
	O1	0.392	0.154	0.378	

less than 5 and GOF must approach to unity [14–16]. In the present case, the χ^2 and GOF values were found to be well less than 5 and nearer to 1 for the above structurally refined ion irradiated phosphor.

3.1.3. Unit cell representation

Inset of Fig. 2(a) illustrates an Y_2O_3 unit cell for virgin phosphor. The unit cell was modeled through a program called Visualization for Electronic and Structural Analysis (VESTA) [16] using Rietveld refinement data from Table 1. The Y_2O_3 phosphor has a cubic structure with a space group (Ia-3) and point-group symmetry (m-3). The unit cell contains 16 formula units with 32 cations. This structure contains two cation symmetry sites C_2 and C_{3i}, both coordinated six-fold with oxygen as shown in the inset of Fig. 2(a). These two cationic sites C_2 and C_{3i} were distributed over two Wyckoff positions 24d and 8b respectively. Oxygen ions were located at 48e Wyckoff positions. The ionic radii of Y^{3+} (0.9 Å) and Dy^{3+} (0.92 Å) are very close, and hence it is possible to substitute Y^{3+} with Dy^{3+} ions and do not cause any change in the cubic structure of the host lattice. Ion irradiation also does not affect the cubic structure of this phosphor.

3.1.4. Transmission electron microscopy

Fig. 3(a–c) depicts the TEM micrograph for virgin, Ni and Ag swift ion irradiated Y_2O_3:Dy^{3+} phosphors for the highest ion fluence of 1×10^{13} ions/cm^2. The corresponding selected area electron diffraction (SAED) patterns are also shown in Fig. 3(d) (i–iii).

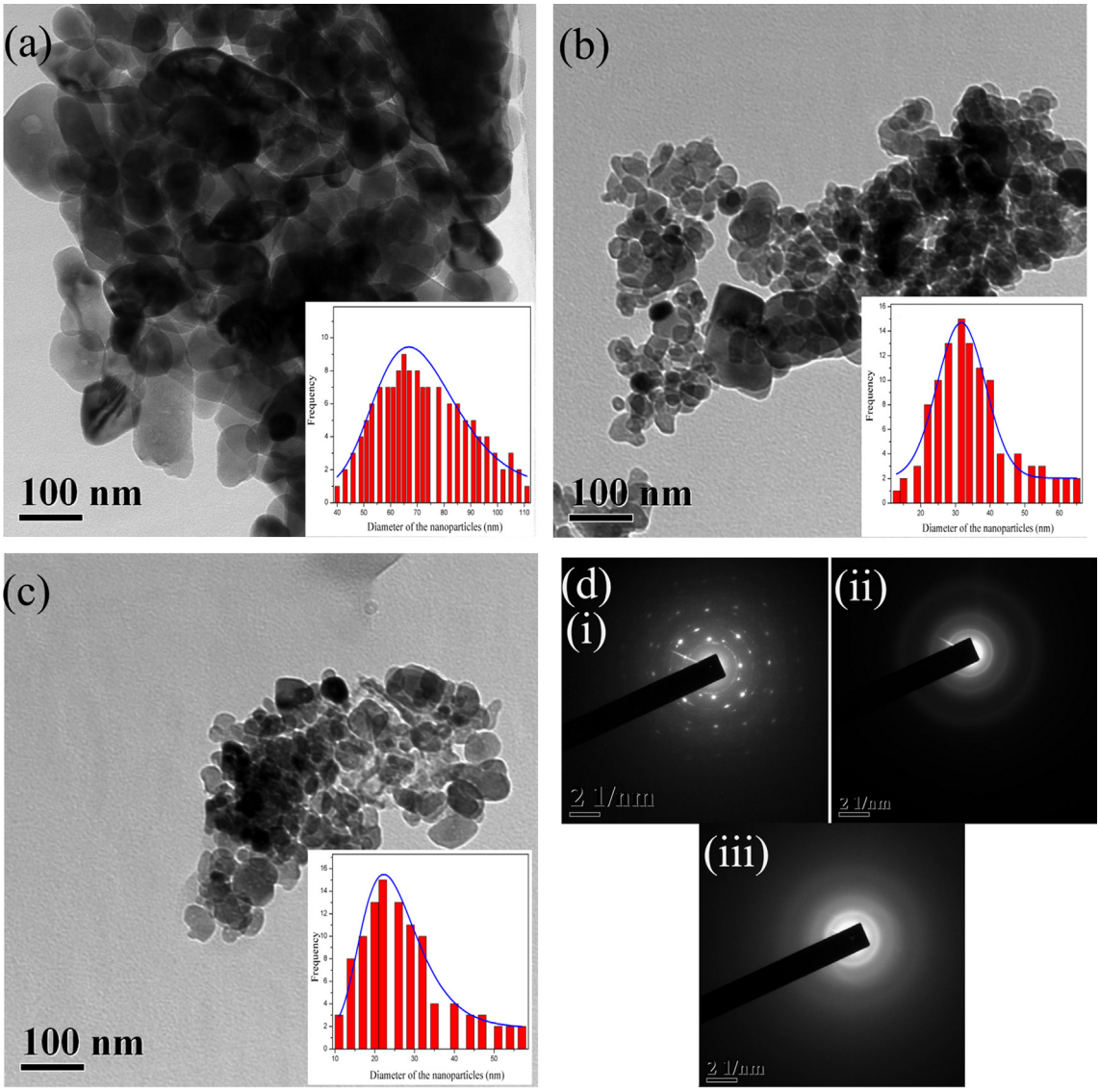

Fig. 3. TEM images for Y_2O_3:Dy^{3+} phosphors.

The change in surface morphology was observed for SHI induced phosphors. SHI irradiation breaks the agglomerated particles into irregular shaped particles with reduced size. The reduction in particle size may be attributed to the fragmentation of larger grains as a result of swift heavy ion irradiation. The SAED pattern of virgin phosphor exhibits the diffraction spots indicating a high degree of crystallinity but after SHI irradiation, diffraction spots change into diffused rings indicating the loss of crystallinity [13]. The loss of crystallinity for SHI induced phosphors is in agreement with XRD results.

The frequency plot of the size distribution, shown in the inset of Fig. 3(a–c) for virgin, Ni, Ag and Au swift ions irradiated Y_2O_3:Dy^{3+} phosphor at the ion fluence of 1×10^{13} ions/cm^2 was obtained by measuring the size of a large number of particles in each phosphor. Size distribution for the particles were found to obey log normal nature [17]

$$P(d) = \frac{1}{d\sigma\sqrt{2\pi}} exp\left[\frac{-ln^2(d/\overline{d})}{2\sigma^2}\right] \quad (1)$$

here d and σ are related to the average size and the size distribution of the particles. By fitting the frequency plot using Eq. (1) [solid blue line in Figure], the average particle size of virgin phosphor was estimated to be 67 nm with a narrow size distribution ($\sigma = 0.20$). The average particle size of Ni and Ag ions irradiated phosphors was found to be 28 and 24 nm with a wider size distribution ($\sigma = 0.24$ and 0.28) respectively.

3.2. Diffuse reflectance studies

The diffuse reflectance (DR) spectra of virgin and ion irradiated Dy^{3+} doped Y_2O_3 powder phosphor were recorded against a reference standard spectralon (Fig. 4). Fig. 4(a) shows the DR spectra of virgin phosphor. A sharp absorption band at 213 nm was observed for virgin sample confirming that light having this particular wavelength was absorbed by this phosphor. This band was due to band gap of the virgin phosphor. The other bands present in the DR spectra were due to meta-stable energy states

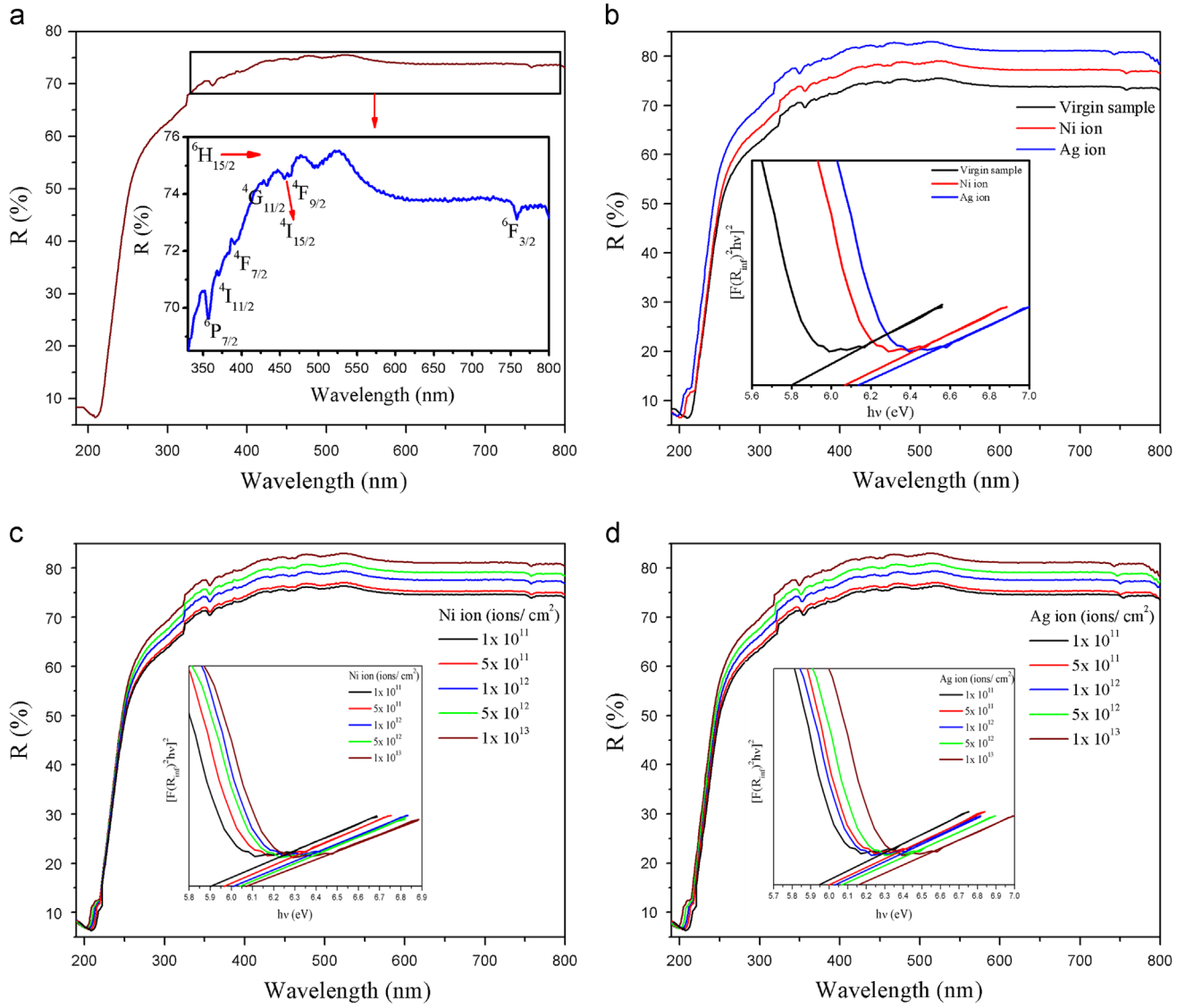

Fig. 4. DR spectra of virgin and SHI irradiated Y_2O_3:Dy^{3+} phosphors.

formed in between valence and conduction bands by the Dy^{3+} ions. These transitions are shown in the inset of the Fig. 4(a). Fig. 4(b) shows the Ni and Ag ion irradiation effects on DR spectra of Y_2O_3:Dy^{3+} phosphor for maximum ion fluence 1×10^{13} ions/cm^2. In case of ion irradiated samples, the absorption band shifts toward blue region. For Ag ion irradiated phosphor this shift is more. Fig. 4(c) and (d) shows the DR spectra of Ni and Ag ion irradiated phosphors for varying ion fluences. It shows the shift in main absorption band toward lower wavelength region. But no shift was observed for the other weak bands present in the irradiated phosphors. This interesting phenomenon may be due to the fact that both the ground state (4f) and excited state (5d) of Dy^{3+} changes in such a way that the energy separation between these levels does not change [10].

Table 2
Bandgap of virgin and ion irradiated Y_2O_3:Dy^{3+} phosphors.

Phosphors	Fluence (ions/cm^2)	Bandgap (eV)
Virgin	–	5.8
Ni ion irradiated	1×10^{11}	5.9
	5×10^{11}	5.97
	1×10^{12}	6.01
	5×10^{12}	6.04
	1×10^{13}	6.07
Ag ion irradiated	1×10^{11}	5.95
	5×10^{11}	6.00
	1×10^{12}	6.03
	5×10^{12}	6.07
	1×10^{13}	6.17

3.3. Bandgap

The Kubelka–Munk theory [18] was used to calculate the band gap of virgin and ion irradiated phosphors from DR spectra. In DR spectra, the ratio [18] of the light scattered from a thick layer of sample and an ideal non-absorbing reference sample is measured as a function of the wavelength λ,

$R_\infty = R_{sample}/R_{reference}$. The relation between diffuse reflectance of the sample (R_∞), absorption coefficient (K) and scattering coefficient (S) is given by the Kubelka–Munk function $F(R_\infty)$

$$F(R_\infty) = \frac{(1-R_\infty)^2}{2R_\infty} = \frac{K}{S} \quad (2)$$

The direct band gap E_g and linear absorption coefficient α of a material is related through the well-known Tauc relation

$$\alpha h\nu = C_1(h\nu - E_g)^{1/2} \quad (3)$$

here $h\nu$ is the photon energy and C_1 is a proportionality constant. When the material scatters in perfectly diffuse manner (or when it is illuminated at 60° incidence), the absorption coefficient K becomes equal to 2α. Considering the scattering coefficient S as constant with respect to wavelength, and using Eqs. (2) and (3), the following expression can be obtained:

$$[F(R_\infty)h\nu]^2 = C_2(h\nu - E_g) \quad (4)$$

From the plot of $[F(R_\infty)h\nu]^2$ versus $h\nu$ as shown in the inset of Fig. 4(b–d), the value of E_g was obtained by extrapolating the linear fitted regions to $[F(R_\infty)h\nu]^2 = 0$. The band gap calculated from the DR spectra using K–M function $F(R_\infty)$ for virgin phosphor was found to be 5.8 eV. For Ni^{7+} irradiated phosphor, the bandgap varies from 5.9 eV to 6.07 eV and for Ag^{9+} irradiated phosphor, it was seen to vary from 5.95 eV to 6.16 eV with ion fluence. This indicates that the tunning of bandgap is possible after swift heavy ion irradiation. At the same ion fluence, the Ag ion irradiated phosphor has greater bandgap than the Ni ion irradiated phosphor. The calculated bandgap is summarized in Table 2.

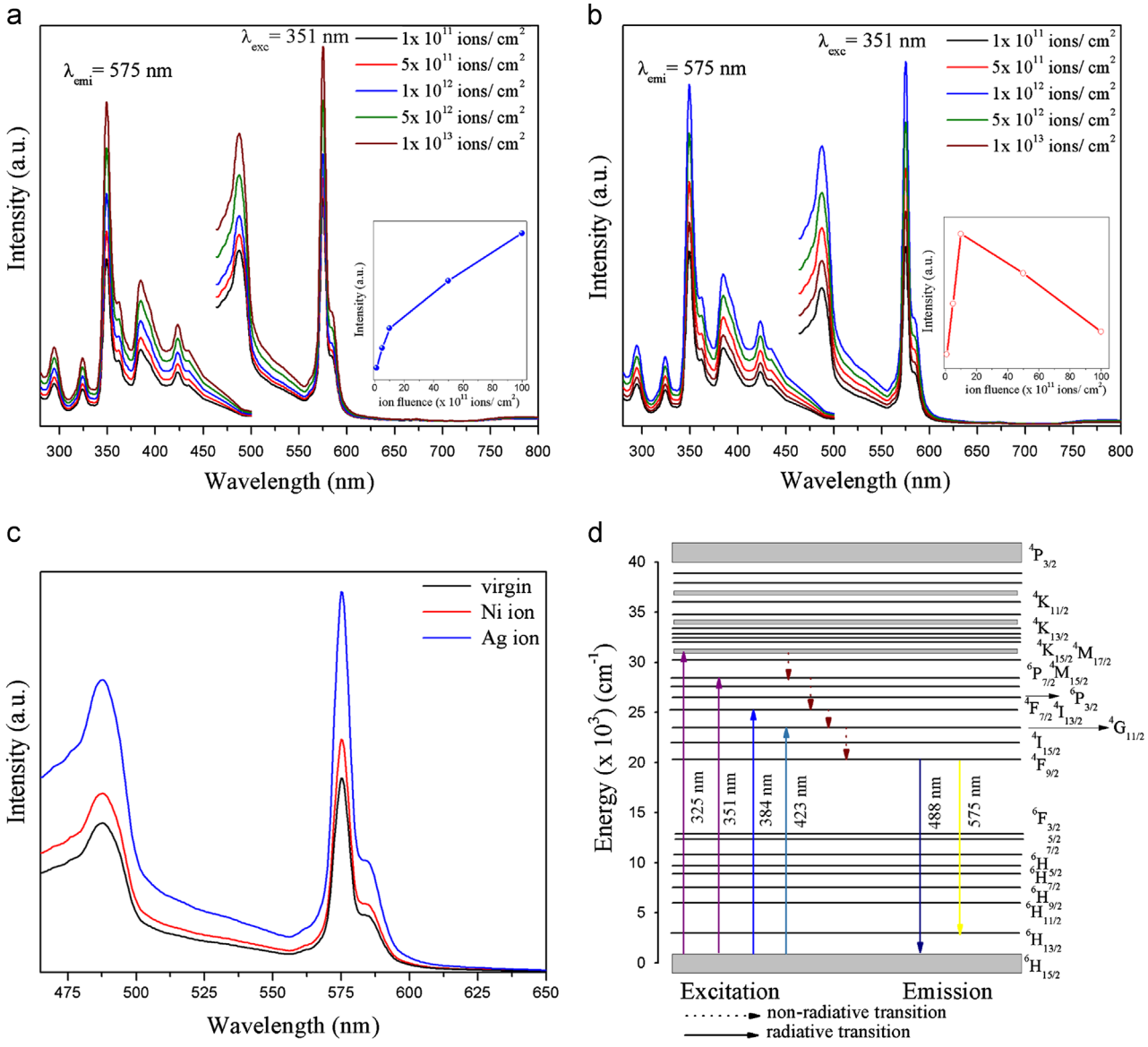

Fig. 5. PL spectra of virgin and SHI irradiated Y_2O_3:Dy^{3+} phosphors.

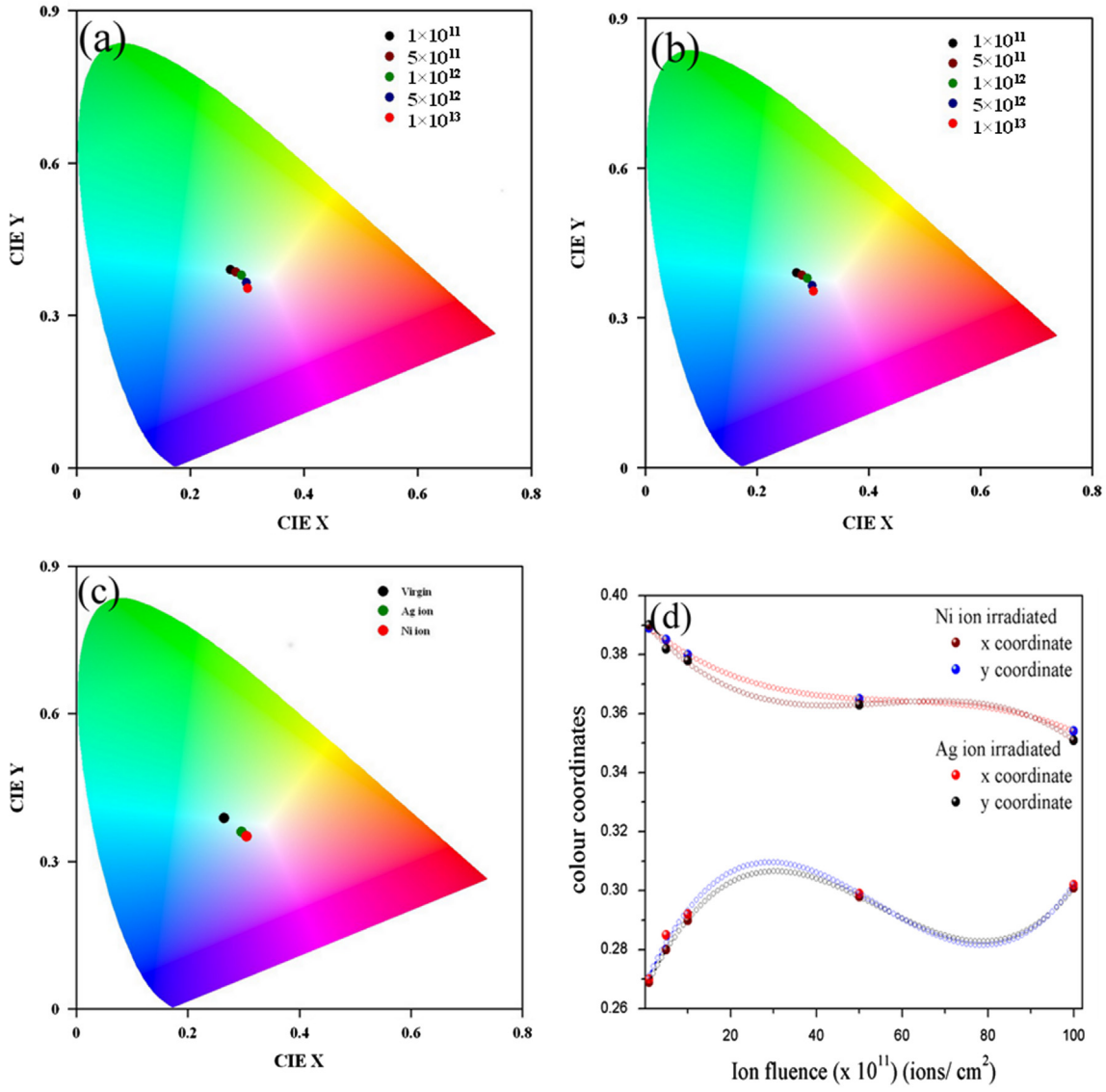

Fig. 6. CIE diagram of virgin and SHI irradiated Y_2O_3:Dy^{3+} phosphors.

3.4. Photoluminescence studies

Fig. 5(a,b) shows the photoluminescence (PL) emission and excitation spectra of Ni and Ag ion irradiated phosphors at different ion fluences. The emission spectra were recorded at excitation wavelength of 351 nm. The 351 nm radiation excites the Dy^{3+} ions from ground state to the higher excited state $^6P_{7/2}$ level and then quickly relaxes to $^4F_{9/2}$ level by emitting nonradiative transitions. The strong yellow emission band centered at 575 nm corresponds to the hypersensitive transition $^4F_{9/2} \rightarrow {}^6H_{13/2}$. Another feeble blue emission band at 488 nm corresponds to the $^4F_{9/2} \rightarrow {}^6H_{15/2}$ transition, which is less sensitive to the host. The reason behind observing the intense yellow emission from Y_2O_3:Dy^{3+} can be understood by considering the structure of Y_2O_3. The coordination number of Y_2O_3 is six and forms cubic bixbyite structure with two different sites (C_2 and C_{3i}) for RE^{3+} ions substitution. The C_2 is a low symmetry site without an inversion center whereas C_{3i} is a high symmetry site having an inversion center. When Dy^{3+} is located at a low symmetry (C_2), the yellow emission is dominant whereas the blue emission is dominant when Dy^{3+} is located at a high symmetry (C_{3i}) [6]. In the present case, yellow emission is dominant suggesting that the location of Dy^{3+} is more favorable at C_2 site. As the C_2 site does not have an inversion center, electric dipole transitions from Dy^{3+} ions attached to this site are more favorable than the magnetic dipole transitions. The similarity of the ionic radii of Dy^{3+} and Y^{3+} ions allows the easy substitution of Y^{3+} ions with Dy^{3+} ions at C_2 sites giving rise to intense yellow emissions in all the samples. The inset of Fig. 5(a and b) shows the variation of PL intensity with ion fluence for both the ions.

With the increase in ion fluence, the PL intensity increases for Ni irradiated phosphors indicating an increase in color centre formation with ion fluence. But for Ag ion irradiated phosphor, the PL intensity increases upto ion fluence 1×10^{12} ions/cm^2 and then decreases. This may be attributed to irradiation induced

Table 3
CIE parameters of virgin and ion irradiated Y_2O_3:Dy^{3+} phosphors.

Phosphors	Color coordinates		CCT	CRI	LER	Value	Ni ion		Ag ion	
	x	y	(K)	(R_a)			x	y	x	y
Virgin	0.265	0.388	8199	33	302	A	0.266	0.39	0.268	0.391
Ni (1×10^{13})	0.301	0.354	6904	21	335	B	0.003	−0.001	0.003	−0.002
Ag (1×10^{13})	0.302	0.351	6882	19	338	C	-6.9×10^{-5}	1.9×10^{-5}	-7.6×10^{-5}	3.2×10^{-5}
						D	4.3×10^{-7}	-1.1×10^{-7}	4.7×10^{-7}	-1.9×10^{-7}

amorphization as a result of cascade quenching at higher fluence [19]. Ag ions having ion fluence greater than 1×10^{12} ions/cm^2 may create one or several displacement cascades, which become amorphous as a result of rapid quenching, and these cascades eventually overlap to form an amorphous solid [19].

Fig. 5(c) shows the comparison graph for PL emission of virgin, Ni and Ag ion irradiated phosphors for ion fluence 1×10^{11} ions/cm^2. It shows that after ion irradiation PL intensity increases drastically. The PL intensity is sensitive to the damage created by swift heavy ions. A strong PL intensity indicates dominant radiative transitions. As the concentration of the color centers increases, the rate of radiative transition also increases. Furthermore, grain boundaries acts as color centers, fragmentation caused by SHIs increases the density of these grain boundaries which increases the PL emission intensity. But more fragmentation quenches the luminescence intensity as for the case of Ag ion irradiated sample after irradiation by ion fluence 1×10^{12} ions/cm^2.

Excitation spectra were recorded keeping the emission wavelength fixed at 575 nm (Fig. 5(a and b)). These spectra consists of several excitation bands of f–f transitions, which are ascribed to the different transitions from the ground state $^6H_{15/2}$ to the various excited states of $4f^9$ electronic configuration of the Dy^{3+} ions. The excitation maxima located at 351 nm corresponds to the hypersensitive transition from the ground $^6H_{15/2}$ to $^6P_{7/2}$ level [6]. All these transitions are shown in the schematic energy level diagram of Dy^{3+} in Y_2O_3 host in Fig. 5(d). The similar behavior of the excitation spectra was also observed with ion fluence as observed in PL emission spectra.

Moreover, blue to yellow (B/Y) intensity ratio (I_{488}/I_{575}) falls in the region 0.72–0.80 for the ion irradiated phosphors. It is expected that pure white light emission can be achieved by controlling suitable B/Y intensity ratio after irradiation by other swift heavy ions of different fluences.

3.5. CIE parameters

Fig. 6(a and b) illustrates the CIE chromaticity diagram of Ni and Ag ion irradiated phosphors for varying ion fluences. Fig. 6 (c) shows the chromaticity diagram of virgin, Ni and Ag ion irradiated phosphor at maximum ion fluence 1×10^{13} ions/cm^2.

The CIE parameters such as color coordinates (x–y), color correlated temperature (CCT), color rendering index (CRI) and luminescence efficacy of radiation (LER) were calculated in order to know the change in the photometric characteristics of Y_2O_3:Dy^{3+} phosphor with ion fluence. The color coordinates (x–y) were calculated using standard procedure. The CCTs of the ion irradiated phosphors were given by the McCamy empirical formula [20]

$$\mathrm{CCT} = -437n^3 + 3601\mathrm{n}^2 - 6861\mathrm{n} + 5514.31 \quad (5)$$

where $n=(x-x_e)/(y-y_e)$ is the inverse slop line, and $x_e=0.3320$ and $y_e=0.1858$ [14]. The other parameters were calculated using the spectral energy distribution of chromaticity diagram [14]. The CIE parameters of virgin and ion irradiated phosphors at maximum ion fluence are summarized in Table 3. The ion fluence dependence of both x and y color coordinates is plotted in Fig. 6(d). The figure shows that the x-coordinate increases and y-coordinate decreases with the increase in ion fluence. These color coordinates are fitted in a cubical polynomial function of the form $f(x)=A+Bx+Cx^2+Dx^3$. The values of coefficients A, B, C and D are given in Table 3. However, the color coordinates of Ni ion irradiated phosphor is more nearer to white light region as compared to Ag ion irradiated phosphor.

4. Conclusions

150 MeV Ni^{7+} and 120 MeV Ag^{9+} ions impart their energy to Y_2O_3:Dy^{3+} phosphor mainly by electronic energy loss which is more in case of Ag ion irradiation. XRD studies show that the structure of the phosphors does not change but loses its crystallinity after ion irradiation and the loss of crystallinity is greater in case of Ag ion irradiated phosphor. TEM studies show that the ion irradiation breaks the agglomerated particles into irregular shaped particle with reduced size. The clear diffraction spots turns into diffuse rings confirming the loss in crystallinity after heavy ion irradiation. The modification/ rearrangement of color/luminescent centre also take place causing an increase in luminescence intensity. The tunability of color emission and bandgap was achieved after ion irradiation. It may be exploited in tunable laser, solid state lighting and various optoelectronic devices.

Acknowledgment

The authors are thankful to University Grants Commission, New Delhi, Government of India for funding this work (Project F. No. 37-200/2009 (SR)).

References

[1] G. Agarwal, V. Kulshrestha, R. Dhunna, D. Kabiraj, S. Verma, I.P. Jain, Study of intermixing and Zr-silicide formation using swift heavy ion irradiation, Applied Physics A 99 (2010) 879–888.

[2] K. Jeet, V.K. Jindal, L.M. Bharadwaj, D.K. Avasthi, K. Dharamvir, Damaged carbon nanotubes get healed by ion irradiation, Journal of Applied Physics 108 (034302) (2010) 1–6.

[3] V. Kumar, R. Kumar, S.P. Lochab, N. Singh, Effect of swift heavy ion irradiation on nanocrystalline CaS:Bi phosphors: structural, optical and luminescence studies, Nuclear Instruments and Methods in Physics B 262 (2007) 194–200.

[4] G.A. Kachurin, S.G. Cherkova, D.V. Marin, A.G. Cherkov, V. A. Skuratov, Light-emitting Si nanostructures formed in silica layers by irradiation with swift heavy ions, Applied Physics A 98 (2010) 873–877.

[5] K.R. Nagabhushana, B.N. Lakshminarasappa, F. Singh, Photoluminescence and Raman studies in swift heavy ion irradiated polycrystalline aluminum oxide, Bulletin of Materials Science 32 (5) (2009) 515–519.

[6] M. Jayasimhadri, L.R. Moorthy, K. Kojima, K. Yamamoto, N. Wada, N. Wada, Optical properties of Dy^{3+} ions in alkali Tellurophosphate glasses for laser materials, Journal of Physics D: Applied Physics 39 (2006) 635–641.

[7] D. Severin, E. Balanzat, W. Ensinger, C. Trautmann, Outgassing and degradation of polyimide induced by swift heavy ion irradiation at cryogenic temperature, Journal of Applied Physics 108 (2010) 024901-1–024901-5.

[8] W. Bolse, B. Schattat, A. Feyh, Modification of thin-layer systems by swift heavy ions, Applied Physics A 77 (2003) 11–15.

[9] N. Vu, T.K. Anh, G. Yi, W. Strek, Photoluminescence and cathodoluminescence properties of Y_2O_3: Eu nanophosphors prepared by combustion synthesis, Journal of Luminescence 122-123 (2007) 776–779.

[10] A. Vij, R. Kumar, A.K. Chawla, S.P. Lochab, R. Chandra, N. Singh, Swift heavy ion induced synthesis and enhanced photoluminescence of SrS: Ce nanoparticles, Optical Materials 33 (2010) 58–62.

[11] G. Szenes, General features of latent track formation in magnetic insulators irradiated with swift heavy ions, Physical Review B 51 (1995) 8026–8029.

[12] S. Som, S.K. Sharma, Eu^{3+}/Tb^{3+}-codoped Y_2O_3 nanophosphors: Rietveld refinement, bandgap and photoluminescence optimization, Journal of Physics D: Applied Physics 45 (2012) 415102.

[13] S. Som, S.K. Sharma, S.P. Lochab, Swift heavy ion induced structural and optical properties of Y_2O_3:Eu^{3+} nanophosphor, Materials Research Bulletin 48 (2013) 844–851.

[14] H.M. Rietveld, A profile refinement method for nuclear and magnetic structures, Journal of Applied Crystallography 2 (1969) 65–71.

[15] J. Rodriguez-Carvajal, Full Computer Program, ⟨http://www.ill.eu/sites/fullprof/php/downloads.html⟩, 2010.

[16] K. Momma, F. Izumi, VESTA: a three-dimensional visualization system for electronic and structural analysis, Journal of Applied Crystallography, 41 (2008) 653–658.

[17] G. Mitrikas, C.C. Trapalis, G. Kordas, Tailoring the particle size of sol-gel derived silver nanoparticles in SiO_2. Journal of Non-Crystalline Solids 286 (2001) 41–50.

[18] A.E. Morales, E.S. Mora, U. Pal, Use of diffuse reflectance spectroscopy for optical characterization of un-supported nanostructures, Revista Mexicana de Física 53 (5) (2007) 18–22.

[19] H. Nagabhushana, B.N. Lakshminarasappa, F. Singh, D.K. Avasthi, Photoluminescence studies in swift heavy ion bombarded mullite, Nuclear Instruments and Methods in Physics B 211 (2003) 545–548.

[20] G.A. Kumar, M. Pokhrel, A. Martinez, R.C. dennis, I.L Villegas, D. K. Sardar, Synthesis and spectrβoscopy of color tunable Y_2O_2S:Yb^{3+}, Er^{3+} phosphors with intense emission, Journal of Alloys and Compounds 513 (2012) 559–565.